Eur Biophys J (2005) 34: 294–305
DOI 10.1007/s00249-004-0455-7

ARTICLE

Marja T. Hyvönen · Petri T. Kovanen

Molecular dynamics simulations of unsaturated lipid bilayers: effects of varying the numbers of double bonds

Received: 2 April 2004 / Accepted: 5 December 2004 / Published online: 2 February 2005

Abstract The importance of unsaturated, and especially polyunsaturated phosphatidylcholine molecules for the functional properties of biological membranes is widely accepted. Here, the effects of unsaturation on the nanosecond-scale structural and dynamic properties of the phosphatidylcholine bilayer were elucidated by performance of multinanosecond molecular dynamics simulations of all-atom bilayer models. Bilayers of dipalmitoylphosphatidylcholine and its mono-, di-, and tetraunsaturated counterparts were simulated, containing, respectively, oleoyl, linoleoyl, or arachidonoyl chains in the *sn*-2 position. Analysis of the simulations focused on comparison of the structural properties, especially the ordering of the chains in the membranes. Although the results suggest some problems in the CHARMM force field of the lipids when applied in a constant pressure ensemble, the features appearing in the ordering of the unsaturated chains are consistent with the behaviour known from ^{2}H NMR experiments. The rigidity of the double bonds is compensated by the flexibility of *skew* state single bonds juxtaposed with double bonds. The presence of double bonds in the *sn*-2 chains considerably reduces the order parameters of the CH bonds. Moreover, the double bond region of tetraunsaturated chains is shown to span all the way from the bilayer centre to the head group region.

Keywords Membrane · Phospholipid · Polyunsaturation · Orientational order parameter · Conformation

M. T. Hyvönen · P. T. Kovanen
Wihuri Research Institute, Kalliolinnantie 4,
00140 Helsinki, Finland

M. T. Hyvönen (✉)
Laboratory of Physics and Helsinki Institute of Physics,
Helsinki University of Technology, P.O. Box 1100,
02015 Helsinki, Finland
E-mail: marja.hyvonen@wri.fi
Tel.: + 358-9-6814132
Fax: + 358-9-637476

Introduction

Double bonds of the unsaturated fatty acyl chains are known to heavily modify the properties of biological membranes. Accordingly, their presence in the fatty acyl chains of membrane-forming phospholipids is an essential and strictly regulated property of all mammalian cells. The state of the double bonds in natural phosphatidylcholine (PC) molecules is *cis*, causing bending of the hydrocarbon chain. Therefore, the double bond affects the structural and dynamical properties of the other parts of the chains, thereby affecting the overall properties of the whole membrane. Major effects of unsaturation have been reported to be the increase in area per lipid and the decrease in transition temperature between gel and liquid-crystalline phases (Demel et al. 1972; Evans et al. 1987; Stillwell and Wassal 2003), both effects appearing most significant after the introduction of the first double bond. Despite the increasing amount of information on the effects of double bonds on lipid molecular systems, information on direct structural and dynamic effects is still scarce. Many experimental observations remain to be interpreted, and their in-depth understanding requires information difficult or even impossible to obtain experimentally. For instance, an interesting issue in the field of membrane research is the phenomenon of passive permeation through lipid membranes in relation to changes in the lipid unsaturation state (Demel et al. 1972; Fettiplace and Haydon 1980; In't Veld et al. 1992; Huster et al. 1997; Zeng et al. 1998).

During the last decade, the molecular dynamics (MD) simulations of lipid membranes increasingly employed have provided in-depth information on lipid systems and molecular level explanations for a variety of experimentally observable phenomena (Pastor 1994; Tobias et al. 1997; Bandyopadhyay et al. 1998; Feller 2000). Although the research field of MD simulations of lipid systems is still young, the number of simulations assessing relevant problems is rapidly increasing, to-

gether with improving quality. To be able to simulate physiologically relevant lipid systems, unsaturated lipids need to be incorporated. However, before mixing of different lipid species, they should be simulated as such to allow assessment of possible problems in the force fields and in other MD methodology. Such simulations also provide the essential basic information on the behaviour and properties of these different lipid species further needed in assessing results for compositionally more complex systems.

Earlier MD simulation studies on unsaturated systems include reports on PC bilayers with monounsaturated chains (Heller et al. 1993; Huang et al. 1994; Ceccarelli and Marchi 1998; Murzyn et al. 2001; Rabinovich et al. 2003; Rog et al. 2004), on 1-palmitoyl-2-linoleoyl-*sn*-glycero-3-phosphatidylcholine (PLPC) bilayers containing diunsaturated linoleic acyl chains (Hyvönen et al. 1995, 1997a, 1997b; Bachar et al. 2004), and on PCs with docosahexaenoyl chains with six double bonds (Huber et al. 2002; Saiz and Klein 2001a, 2001b; Feller et al. 2002; Rabinovich et al. 2003). Here, MD simulations are applied in the elucidation of the properties of four distinct bilayers consisting of variably unsaturated PC molecules, namely 1,2-dipalmitoyl-*sn*-glycero-3-phosphatidylcholine (DPPC, 16:0/16:0), 1-palmitoyl-2-oleoyl-*sn*-glycero-3-phosphatidylcholine (POPC, 16:0/18:$1^{\Delta 9}$), PLPC (16:0/18:$2^{\Delta 9,12}$), and 1-palmitoyl-2-arachidonoyl-*sn*-glycero-3-phosphatidylcholine (PAPC, 16:0/20:$4^{\Delta 5,8,11,14}$). Of these, DPPC is a fully saturated reference system, whereas POPC, PLPC, and PAPC have one, two, and four double bonds in their *sn*-2 chains. Accordingly, this work is a systematic computational study to assess the effects of a gradual increase in the number of double bonds. While the saturated DPPC molecule is the well-documented benchmark lipid, the others are important natural constituents of biological membranes. Indeed, oleoyl phospholipids and linoleoyl phospholipids have been claimed to be the most prevailing phospholipid species in various cell membranes and arachidonoyl phospholipids play an important role, for instance, in the membranes of T cells (Tomita et al. 2004). Interestingly, the arachidonoyl residue also plays a role as a constituent of an endocannabinoid 2-arachidonoyl glycerol (Walter and Stella 2003). Each of the fatty acids studied here is found, for instance, in low-density lipoproteins (LDL) (Esterbauer et al. 1990), and furthermore, the oxidized form of PAPC from LDL has been suggested to have various atherosclerosis-related effects in human vascular endothelial cells (Walton et al. 2003; Birukov et al. 2004, and references therein). Altogether, there is a wealth of information on the physiological effects of the various naturally occurring fatty acids. In contrast, molecular level information of the structural and functional properties is often scarce, so hindering in-depth understanding of the pathology of living systems, which is essential in the elucidation of new possibilities to pharmacologically affect specific molecular mechanisms of cells.

Methods

Modelling and computational details

The PC molecules used to construct the bilayer models consist of a glycerol backbone (C1–C3, interfacial region) into which the saturated palmitic acid chain (16:0) and the PC head group are attached to the positions *sn*-1 and *sn*-3, respectively (Fig. 1). To the *sn*-2 position are attached the variably unsaturated chains, i.e., saturated palmitoyl in the DPPC molecule, monounsaturated oleoyl 18:$1^{\Delta 9}$ in the POPC molecule, diunsaturated linoleoyl 18:$2^{\Delta 9,12}$ in the PLPC molecule, and tetraunsaturated arachidonoyl 20:$4^{\Delta 5,8,11,14}$ in the PAPC molecule. The PLPC bilayer came directly from our previous simulation (Hyvönen et al. 1997a) and consists of 72 lipid molecules in a bilayer with 2,572 hydrating water molecules (approximately 35 water molecules per lipid). Construction of the POPC and DPPC bilayers was based on the PLPC system. For DPPC, two carbon segments from the *sn*-2 chains were removed and the necessary hydrogens added to the earlier double-bonded carbons. For POPC, only the second double bond was

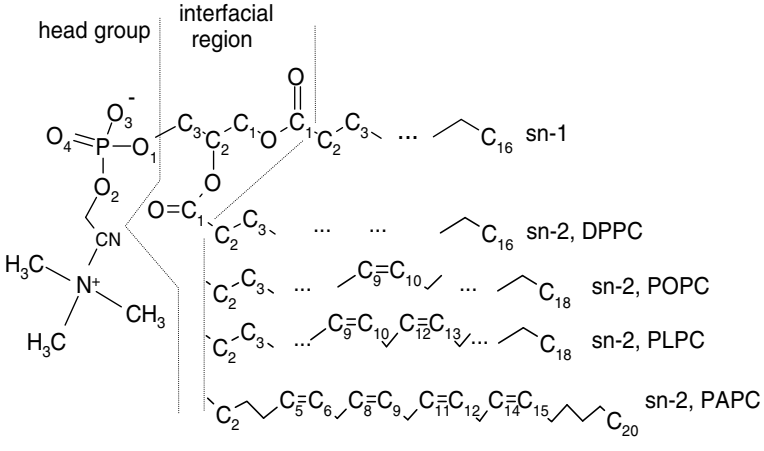

Fig. 1 Molecular structures of 1,2-dipalmitoyl-*sn*-glycero-3-phosphatidylcholine (*DPPC*), 1-palmitoyl-2-oleoyl-*sn*-glycero-3-phosphatidylcholine (*POPC*), 1-palmitoyl-2-linoleoyl-*sn*-glycero-3-phosphatidylcholine (*PLPC*), and 1-palmitoyl-2-arachidonoyl-*sn*-glycero-3-phosphatidylcholine (*PAPC*) indicating atom numbering and names of molecular groups

replaced by a single bond and the necessary two hydrogens added. Before the MD simulation was initiated, these adjustments were followed by energy minimizations. However, in the case of PAPC this procedure was not used. Instead, a group of four PLPC molecules was extracted, where the *sn*-2 linoleoyl chains were manually transformed to arachidonoyl chains. This meant adding two extra carbon segments and transforming C5-C6, C8-C9, C11-C12, and C14-C15 bonds to double bonds and C9-C10 and C12-C13 to single bonds. Additionally, the conformation of double bonds was set to *cis*. This block of four molecules was then energy-minimized and replicated in plane to produce a monolayer of 36 lipid molecules. This monolayer was energy-minimized and replicated to construct a bilayer of 72 PAPC molecules. The water molecules of the PLPC bilayer system were copied to hydrate the PAPC molecules. The 72-molecule section of the bilayer served to model an infinite bilayer through application of periodic boundary conditions. The final energy minimization was reached by first stabilizing the water molecules and then the whole system. The molecular systems consisted of a total of more than 17,000 atoms each. In POPC, PLPC, and PAPC bilayers, the velocities of the atoms were assigned to reach the temperature of 310 K. For the DPPC system, however, a temperature of 323 K was assigned for that bilayer to also attain a liquid–crystalline state. Thereafter, the simulations were initiated using the leapfrog Verlet algorithm with a time step of 1.4 fs. Furthermore, the simulations were carried out for 4.2, 2.9, 2.2, and 3.5 ns for DPPC, POPC, PLPC, and PAPC systems. The temperature and energy components and the dimensions of the systems were monitored during the simulations to ensure their stability and an adequate length of the period for collecting data for analysis. The simulations were stopped after 1 ns of equilibrated period. The evolutions of the dimensions of the primary simulation box are shown in Fig. 2 for each system, together with the area per lipid. Also the average areas per lipid are provided from the last 1 ns. The primary model systems appear as snapshots from the end of the simulations in Fig. 3. The simulations were performed with a fully flexible simulation box in a normal temperature and pressure ensemble to maintain constant temperature and an isotropic pressure of 1 atm with the Nose–Hoover thermostat (Hoover 1985) and a Langevin piston (Feller et al. 1995). The piston collision frequency was 5 ps^{-1}, and the masses of the pressure and thermal pistons were 500 amu and 1,000 kcal ps^2.

The simulation was performed by applying the CHARMm software (CHARMm version 27) (Brooks et al. 1983), and lipid force field parameters were used

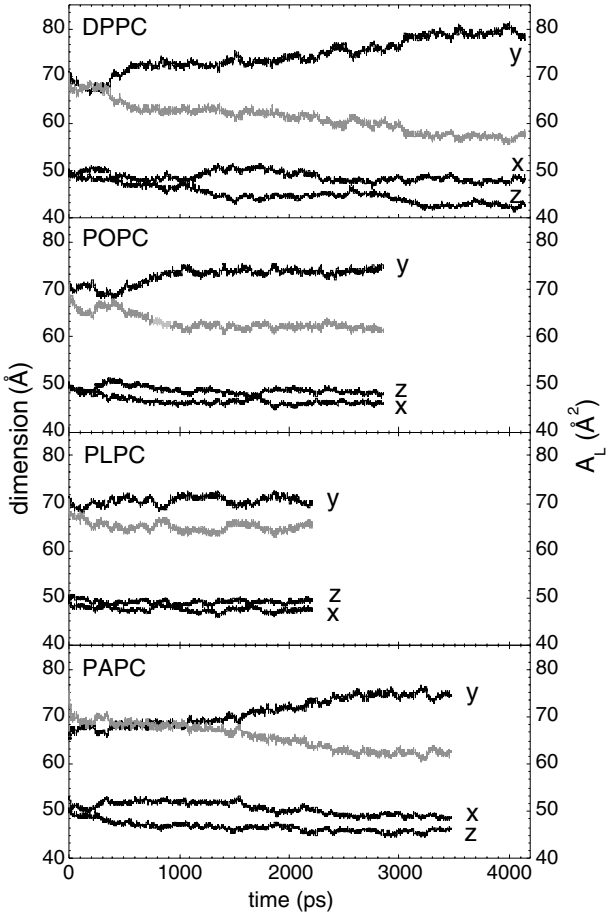

Fig. 2 Dimensions of primary simulation boxes of DPPC, POPC, PLPC, and PAPC bilayer systems, together with the area per lipid (A_L) as a function of time. The average areas per DPPC, POPC, PLPC, and PAPC from the last 1 ns of each simulation are 57.4∓0.6 Å^2, 62.1∓0.5 Å^2, 64.8∓0.8 Å^2, and 62.4∓0.6 Å^2. Note that here dimension *y* is the normal of the bilayer

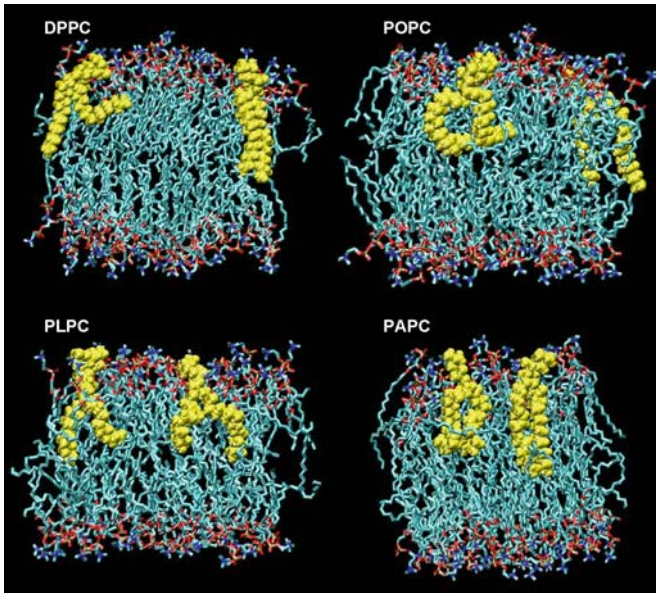

Fig. 3 Snapshots of the primary simulation boxes at the end of the simulations of DPPC, POPC, PLPC, and PAPC bilayer systems. The colour-coding of the lipid molecules is as follows: *cyan* for carbon, *red* for oxygen, *yellow* for phosphorus, and *blue* for nitrogen. In each bilayer two selected conformations are yellow. For clarity, no water molecules or hydrogen atoms are included. The *y*-axis is normal to the membrane

(Schlenkrich et al. 1996; Feller and MacKerell 2000). The CHARMM parameters for the polyunsaturated lipids were published only after the initiation of the present simulations (Feller et al. 2002), but were already available for downloading earlier (http://www.pharmacy.umaryland.edu/faculty/amackere/force_fields.htm). This force field has been utilized in many simulation studies (Saiz and Klein 2001a, 2001b; Feller et al. 2002; Koubi et al. 2003; Eldho et al. 2003; Jensen et al. 2004), and despite the conclusion of too-low areas per lipid in the case of the isobaric ensemble, which also applies to saturated DPPC, the force field has been able to capture the important features of unsaturated lipids. Recent studies imply that this force field should be applied only with a fixed surface area to hinder the shrinkage of the membrane to a gel state (Feller et al. 2002; Koubi et al. 2003; Jensen et al. 2004). This information was, however, not available at the time of the simulations presented here. Instead, several reviews had discussed the importance of an isobaric ensemble in membrane simulations (Berendsen and Tieleman 1998; Tobias et al. 1997; Merz 1997; Tieleman et al. 1997; Saiz et al. 2001), which was therefore a natural choice for our simulations, and still is, inasmuch as no reliable values are available for the areas of many lipid species. Overall, the present CHARMM force field has not proved to be suitable for a complete description of variously unsaturated bilayers in constant pressure simulations. For water molecules, the parameters used were TIP3P (Jorgensen et al. 1983). All atoms were independently taken into account in the MD simulation. The lengths of the bonds involving hydrogen atoms were fixed by the SHAKE algorithm. Electrostatic interactions were included via the particle mesh Ewald summation (Darden et al. 1993; Essmann et al. 1995). The Lennard–Jones potential was switched to zero at the region from 10 to 12 Å. The nonbonded-neighbour list, used for calculating the Lennard-Jones potential and the real-space portion of the Ewald sum, was kept until 12 Å and updated every tenth step, similarly to Feller et al. (2002). Energies, coordinates, and velocities were saved at every 50th step.

Data analysis

In the subsequent analysis, the averages were calculated over all saved time steps of production runs (last 1 ns) and over all lipid or water molecules, if not described otherwise.

Atomic single-particle distribution functions in the bilayer normal direction were evaluated by calculating the total amount of each atom in 0.25-Å slices. All distributions were averaged over time. Further, they served to calculate the total mass and electron density across the bilayer. The mean cosine of the angle between the water dipole moment vector and the bilayer normal was also calculated in 0.25-Å slices along the bilayer normal. A zero value results for a random orientation and, here, a positive value corresponds to the orientation of the dipole towards the bilayer centre. The orientation angle of the head group and the glycerol backbone with respect to the bilayer normal as well as the various angle distributions of varying bonds and vectors in the chains were determined by use of 1° slices. The fraction of free volume in the bilayer was estimated according to Marrink et al. (1996a), except that here the total amount of empty volume was not extrapolated, but instead, the free volume accessible for spherical penetrants of varying radius were calculated (until the minimum of 0.1-Å radius). Here, only the free volume profiles for the minimum penetrant size are shown. The grid size was 40×32×40 Å^3 with 0.8-Å spacing, resulting in 100,000 grid points. Full analysis of the free volume in these systems, including the shape distribution, would be very helpful but clearly is beyond the scope of this particular study. Work aiming at a full description is presently under way. The electrostatic potential profile along the bilayer normal y was calculated on the basis of Poisson's equation

$$\psi(y) - \psi(0) = -\frac{1}{\varepsilon_0}\int_0^y \int_0^{y'} \rho(y'')\mathrm{d}y''\mathrm{d}y',$$

where $\psi(y)$ is the electrostatic potential, $\rho(y)$ is the charge density at y, and ϵ_0 is the vacuum permittivity. The charge density was determined in 0.25-Å slices and averaged from the monolayers. The position $y=0$ resides in the middle of the bilayer.

The orientational order is described by the order parameter S_j, which is defined as

$$S_j = \frac{1}{2}\left\langle 3\cos^2\beta_j - 1\right\rangle,$$

where β_j is the angle between the orientation vector and the reference direction. The brackets denote both the ensemble and the time averages. A ^{2}H NMR observable order parameter, S_j^{CD}, is obtained by defining the orientation vector along the CH_j bond, and the bilayer normal as the reference direction. According to this definition we calculated the order parameters for the CH bonds of unsaturated carbon atoms, and, in the case of saturated carbon atoms for the two CH bonds. As an error estimation, the standard error of the mean of the 72 molecular averages is given. For each of the molecules, the molecular average was evaluated from the whole time series of 1 ns. In this way, the effect of high correlation between consecutive time steps is eliminated, which results in more realistic error estimates. It is conventional in MD simulations, especially in united-atom models, to define the orientation vector along the normal of the HC_jH plane or from C_{j-1} to C_{j+1}, which leads to the molecular order parameter S_j^{mol}. When isotropic rotations around the HC_jH plane normal are assumed, the CH bonds and corresponding S_j^{CD} values become equivalent, and S_j^{CD} can be compared with the S_j^{mol} values according to the relation $-2S_j^{\mathrm{CD}} = S_j^{\mathrm{mol}}$

(Seelig and Niederberger 1974). S_j^{mol} may vary between $-1/2$ and 1, corresponding to the variation between perpendicular (90°) and parallel (0°) orientation with respect to the bilayer normal. Usually, a zero value of S_j indicates isotropic orientation distribution, but also, for instance, a single orientation angle of 54.7° in the sample results in a zero value.

The fractions of *skew*$^+$ and *skew*$^-$ states in the single bonds next to double bonds, and the fractions of *gauche*$^+$, *gauche*$^-$, and *trans* states in other single bonds were determined for the dihedral angles of both chains. The division into *skew*$^+$ and *skew*$^-$ states was performed using the ranges 60–180° and −60 to −180°. The division of other single bonds was performed with the ranges −120 to 0° and 0 to 120° for the *gauche*$^+$ and *gauche*$^-$ states, and the rest for the *trans* states. Similar divisions served in evaluation of the rate of isomerization between different states for each bond; the isomerization rate was averaged over molecules.

To characterize the short-scale dynamics, the correlation functions $<\mu(0)\cdot\mu(t)>$ were determined, where μ is the CH vector at various points in the molecule. Calculation of the correlation functions was performed with the CORFUN analysis tool of the CHARMM software (Brooks et al. 1983).

Results and discussion

Equilibration of the simulated molecular system has traditionally been checked by monitoring the evolution of the dimensions of the simulation box. The time series of the dimensions of the simulated bilayer systems shown in Fig. 2 indicate stabilization of the dimensions of the simulation box as well as the area per lipid in this relatively short time scale to allow description of local structural properties. Recently, several studies on bilayer systems that treat carbon segments as united atoms have been able to achieve time scales ranging from tens to hundreds of nanoseconds. They have suggested that bilayer systems equilibrate only at tens of nanoseconds (Anezo et al. 2003; Patra et al. 2003), questioning the validity of the type of all-atom simulations reported here and elsewhere (Saiz and Klein 2001a; Feller et al. 2002; Huber et al. 2002). However, utilization of shorter-scale simulations has been reasoned for describing local short-scale properties, especially in the case of all-atom models, for which longer simulations are often limited, owing to the larger computational cost. Only very recently has a united-atom force field for polyunsaturated PCs been reported (Bachar et al. 2004), and it will allow larger-scale simulations also for these types of lipid molecules. It should be kept in mind, however, that the present atomistic and united-atom descriptions of double bonds may not be able to describe all those features of polyunsaturated membranes that are potentially important for understanding their biological significance. In particular, the suggested hydrogen-bonding propensity of double bonds (Vorobyov et al. 2002) is not described in the present force fields, although such a description could have major impact on the permeation phenomena, for instance. In general, results from simulation studies provide well-reasoned predictions of the properties and behaviour at a qualitative level, and may, but only after careful consideration, also allow quantitative conclusions. Especially in the case of the simulations presented here, care must be taken to consider critically the results in the light of short simulation times.

The areas per lipid in all four systems are 57.4 ∓ 0.6 Å^2, 62.1 ∓ 0.5 Å^2, 64.8 ∓ 0.8 Å^2, and 62.4 ∓ 0.6 Å^2 for DPPC, POPC, PLPC, and PAPC bilayers from the last 1 ns of each simulation. The equilibrated area per lipid of the DPPC bilayer is significantly smaller than the value of 64 Å^2, based on careful evaluation of estimates from various experimental techniques (Nagle and Tristam-Nagle 2000). Although the CHARMM parameter set for phospholipids has been improved (Feller and MacKerell 2000), a very recent report states that the force field will eventually lead to the formation of a gel-state DPPC bilayer in constant-pressure simulations (Jensen et al. 2004), whereas under conditions utilizing a fixed area, performance has been better (Feller and MacKerell 2000; Feller et al. 2002; Sachs et al. 2004). However, as discussed in various review articles, certain advantages lie in the use of a flexible simulation box with constant pressure for membrane simulations (Berendsen and Tieleman 1998; Tobias et al. 1997; Merz 1997; Tieleman et al. 1997; Saiz et al. 2001). As no reliable values for the area per lipid are available for the polyunsaturated lipids simulated here, utilization of a constant-pressure ensemble is a natural choice. On the other hand, a similar 10% underestimation of the area per lipid with the present CHARMM model was reported recently (Saiz and Klein 2001a; Koubi et al. 2003), with the conclusion that important features related to unsaturation are reproducible. As the force field is the same for all the systems described here, a similar type of offset deviation can be expected, which still allows qualitative comparison of the properties of systems and the phenomena resulting from unsaturation of the fatty acids.

Although the increasing area per lipid is usually considered as one of the key effects of unsaturation (Demel et al. 1972; Evans et al. 1987; Stillwell and Wassal 2003), the area does not necessarily successively increase when more double bonds are incorporated, as implied by the results from present simulations, since the area varies in the order DPPC < POPC < PAPC < PLPC. This variation in areas cannot be confirmed on the basis of experimental data, although the molecular areas in the monolayer studies of Evans et al. indicate that, for instance in the series of lipids having 20 carbons in the *sn*-2 chain, the molecular area increases until the incorporation of a third double bond, after which it again drops (Evans et al. 1987). The area per lipid of 65 Å^2 has been utilized in the fixed-area simulation of hexaunsaturated stearoyldocosahexaenoylphosphatidylcholine

(SDPC) bilayers (Feller et al. 2002), based on X-ray experiments (Koenig et al. 1997), which is surprisingly low compared with the 64 Å^2 for totally saturated DPPC (Nagle and Tristam-Nagle 2000). On the basis of that value, it is tempting to assume that the areas per lipid in the polyunsaturated bilayers here fall within the same range. This appears to be premature, however, as experimental results for unsaturated lipids are scarce, and the degree of uncertainty about the values has been high, as extensively discussed by, for instance, Nagle and Tristam-Nagle (2000). Figure 3 offers snapshot views of each simulated bilayer from the ends of the simulations. In each bilayer, two individual lipids with different conformations are shown to illustrate the range of conformational flexibility. For instance, the polyunsaturated chains of PAPC can be found both in very extended and in bent conformations. However, straight and bent conformations are found also in the totally saturated DPPC bilayer, stressing the importance of numerical analysis.

Figure 4 gives a view of the bilayer properties along the bilayer normal as averaged from both monolayers. The distribution of phosphorus atoms is a general marker of membrane thickness, indicating decreasing thickness in the order DPPC > PAPC > POPC > PLPC. In principle, thickness reflects variation in areas per lipid: the greater the area per lipid, the thinner the membrane. The relation between thickness and area is not straightforward, however, as the chain lengths vary in the simulated lipids.

The overlap of distributions of the methyl ends of the chains and the water molecules underlines the idea of membrane flexibility. This flexibility may be necessary for rare improbable phenomena, such as the permeation of small molecules. In fact, this overlap is slightly enhanced in PLPC and PAPC bilayers, as the percentage of chain conformations that bend the methyl end of a chain to the region $y > 10$ Å is approximately 3.5% in DPPC and POPC bilayers, increasing to approximately 6.5% in PLPC and PAPC bilayers.

Distributions of the double bonds across the bilayer become, naturally, wider along with the increasing number of double bonds per chain. In the PLPC bilayer, the distribution of double bonds overlaps slightly the bilayer centre and also the distribution of phosphorus of the head groups, as concluded already in our earlier simulation study on the PLPC bilayer (Hyvönen et al. 1997a) and recent simulations by Bachar et al. (2004) using the new united atom force field for PLPC. Especially notable is, however, the multitude of conformations of the double-bond region of the *sn*-2 arachidonoyl chains to span all the way from the centre to the height of the head group phosphorus.

Interestingly, the distribution of water molecules in the PAPC system was seen to extend as far as approximately 5 Å from the centre of the membrane. This extension was not, however, due to diffusion of water molecules into a highly hydrophobic environment, but instead, one PAPC molecule entered a relatively deep

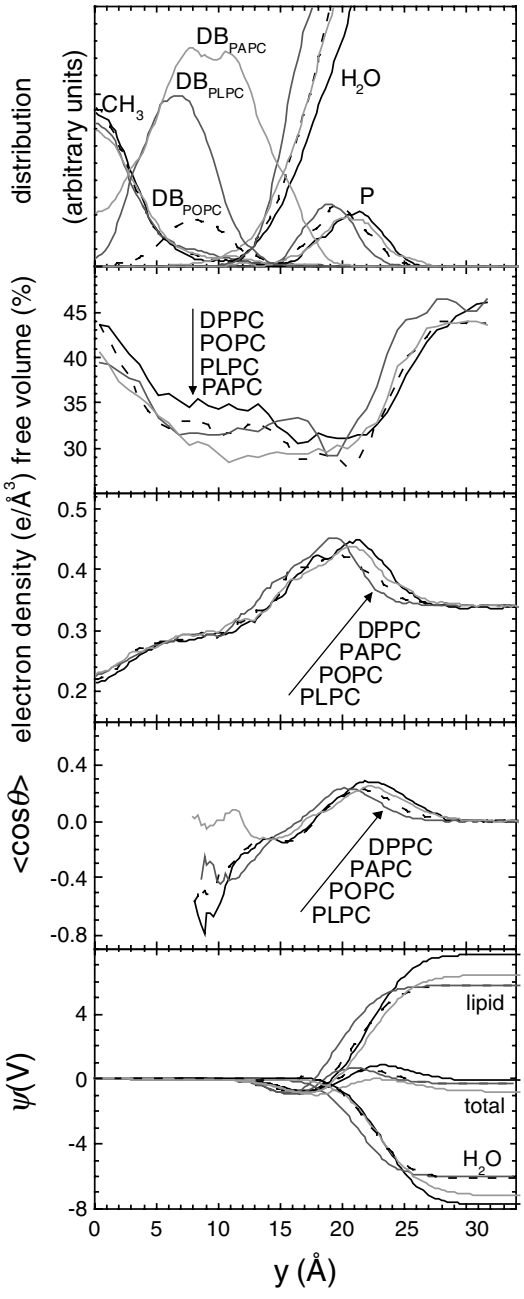

Fig. 4 Atomic distribution functions (*top panel*) of chain methyl (CH_3) and double-bonded (DB) carbon atoms together with water oxygen atoms (H_2O) and the head group phosphorus (P), with distributions in similar units. In addition, the *second panel* shows the fraction of the free volume for a test solute of 0.1-Å dimension along the bilayer normal. The electron density profile, the orientation of water molecules with respect to the bilayer normal, and the electrostatic potential along the bilayer normal are shown in the *three lower panels*. Note that in the *bottom panel* the contributions of lipid and water molecules are presented separately, plus the total potential. The four bilayer systems are as follows: DPPC (*solid black line*), POPC (*broken line*), PLPC (*dark grey line*), and PAPC (*light grey line*). It should be noted also that owing to the relatively short simulation time, phenomena of minor prevalence are also visible in the properties presented

position in the interior, and together with it some water molecules were able to enter there, as well. This kind of phenomenon might have an impact as a possible starting point for the development of hypothetical water pores or wires (Marrink et al. 1996b; Venable and Pastor 2002) or for diffusion of water molecules across the bilayer. In accordance with the findings here, an increase in the water penetration along with the replacement of the 18:1 chain with the 22:6 chain has been reported on the basis of fluorescence lifetime measurements (Mitchell and Litman 1998). The ability of PAPC to move in the bilayer normal direction mentioned earlier may also be a consequence of the increased flexibility of the unsaturated membranes suggested recently by both experimental and simulation studies (Feller et al. 2002; Eldho et al. 2003; Gawrisch et al. 2003). However, as this phenomenon is a single event observed in a short simulation, it necessitates further studies with longer simulation times.

Several experimental studies indicate that the passive permeability and diffusion of small solutes increases along with the incorporation of unsaturated lipids (Demel et al. 1972; Fettiplace and Haydon 1980; In't Veld et al. 1992; Huster et al. 1997; Zeng et al .1998). One straightforward explanation may be an increased fraction of free volume. However, as the second panel of Fig. 4 shows, the fraction of free volume is, on the contrary, merely decreasing along with the unsaturation. This appears to be true especially in the hydrocarbon region where the double bonds reside, and such a decrease is in accordance with the increasing density of the bulk fatty acids in the order palmitic acid < oleic acid < linoleic acid < arachidonoyl acid. In bulk alkenes also, density increases when unsaturation increases. Inasmuch as the phenomenon of increased passive permeability cannot, therefore, be directly explained by the increased free volume, at least in such a short time scale as examined here, longer simulations and more detailed analysis are necessary to address this question thoroughly. The fraction of free volume is largest in the bilayer centre. The minimum amount of free volume appears at the height of head groups in DPPC, POPC, and PLPC bilayers, whereas in PAPC a similar level is also at the height of the upper parts of the chains. Towards the water phase, the fraction of free volume rose to a level also present in the interior of the DPPC bilayer.

Figure 4 also presents the electron density profiles along the bilayer normal, and reveals only minor differences in the bilayer systems, a fact which derives from the different dimensions of the systems. Accordance with the experimental density profiles is good (McIntosh and Simon 1986; Wiener and White 1992). Furthermore, the orientational behaviour of the water molecules (Fig. 4) can be described as the mean cosine of the angle between the water dipole moment vector and the bilayer normal. As stated in earlier simulation studies (Hyvönen et al. 1997a; Hyvönen and Kovanen 2003), the positive peak in the region of the head groups is due to the strong orientation of the hydrogen atoms of the water molecules towards the oxygen atoms of the phosphoryl group. There was an observable difference in the orientation profile of the PAPC system compared with that of the other systems in the region at a distance of approximately 10 Å from the bilayer centre, i.e., at the edge of the region into which water molecules can penetrate. That far from the bilayer surface significantly more water molecules are present in the PAPC bilayer than in the other bilayers, in which the quantity of water is practically zero, and the few counts result merely in a spiky profile. The main orientation of these water dipoles in the DPPC, POPC, and PLPC systems is towards the water surface with ester and phosphoryl oxygens, resulting in negative values. As mentioned, together with one PAPC molecule, water molecules also entered the interior of the bilayer. Those water molecules oriented their dipoles partly towards the ester oxygens of the PAPC molecule that now resides deep in the membrane and partly towards the esters of the neighbouring lipids. This sums up in the merely isotropic overall orientation of the dipole and zero values of the water orientation profile.

The electrostatic potential profiles along the bilayer normal were calculated together with the separate contributions from the lipids and water (Fig. 4, bottom panel). The total potential is negative in the water region compared with that of the interior of the bilayer, with values for the potential of −0.07, −0.32, −0.24, and −0.75 V in the DPPC, POPC, PLPC, and PAPC systems. As reported in other simulation studies, the contribution of lipids is several volts (Feller et al. 1996; Essmann and Berkowitz 1999; Shinoda et al. 1998). This is overcompensated by the orientation of the water molecules, which results in a negative total potential in the water region compared with that of the interior of the bilayer. The experimental values for the potential range from −200 to −575 mV for different phospholipid/water interfaces (Flewelling and Hubbell 1986; Simon and McIntosh 1989; Gawrisch et al. 1992; Simon and McIntosh 1989; Gawrisch et al. 1992; McIntosh et al. 1992). The present simulation results would imply enhanced potential due to unsaturation. However, the experimental values for the potential are scarce, and particularly lacking for unsaturated systems, which makes the validation difficult. Moreover, relatively large differences exist between different experimental techniques (Schamberger and Clarke 2002). Naturally, the relatively small value of the potential in the DPPC bilayer system, compared with the potential values in earlier simulation studies, raises the question how the too-low area per lipid and enhanced packing would affect the overall potential. Recently, Peterson et al. (2002) have speculated as to the effect of packing on the dipole potential and suggested that the disrupted packing should lead to decreased density of lipid dipoles and, subsequently, to a weakened potential. We actually see the opposite effect in the total potential, which is due to the overcompensation caused by water. Accordingly, the

suggestion by Peterson et al. would be applicable in the present study only in the case of the positive potential caused by the lipid molecules: the DPPC with tightest packing and highest dipole density has the largest contribution from the lipids, the contribution being weaker in less packed unsaturated bilayers. In general, the conclusion in the simulation studies has been that the dipole potential is sensitive to the simulation methodology (Anezo et al. 2003; Patra et al. 2003; Berger et al. 1997), and perhaps, therefore, the dipole potential has not always been reported from simulations, making a comparison with recent simulation studies difficult.

The average orientation angles of the phosphorus–nitrogen vector of the PC head groups with respect to the bilayer plane were 20, 17, 17, and 20° in the DPPC, POPC, PLPC, and PAPC systems. These values are in good accordance with the estimated average orientation of 18° in DPPC bilayers from NMR and laser Raman experiments (Akutsu and Nagamori 1991). In the simulations, the distribution of angles was wide (data not shown), from −70 to +90° (negative angle corresponding to orientations towards the bilayer centre). The orientational behaviour of the head groups thus does not differ significantly among various unsaturation states. This conclusion is supported by the similar short-scale relaxation behaviour of a CH vector in the head groups among the different bilayers, as shown later.

Ordering of the fatty acyl chains, described by order parameters in Fig. 5, reflects the excessively low area per lipid in the DPPC bilayer. The *sn*-1 chains of DPPC are considerably more ordered than would be expected from ^{2}H NMR studies (Seelig and Seelig 1974).

In general, the order parameters of both *sn*-1 and *sn*-2 chains decrease owing to unsaturation, an effect naturally much more pronounced in *sn*-2 chains. The order parameter values of the *sn*-1 chains of POPC molecules are significantly lower than those of DPPCs, and the order of PLPCs is even lower. This behaviour is in accordance with the ^{2}H NMR results of Holte et al. (1995). Incorporation of two more double bonds does not, however, reduce the order any further at the same temperature; instead, the order is higher, especially from carbon C7 towards the interior. Although the order parameter profiles of the DPPC bilayer in our simulation otherwise indicated too much order in the chains, the order parameters of 0.11 and 0.14 at position C2 of the *sn*-2 chain of DPPC (only the average in Fig. 5) are in good accordance with the ^{2}H NMR based values of 0.09 and 0.15 of Seelig and Seelig (1974). This detail is, however, seldom reproduced in simulations, which underlines the difficulty in assessing the proper force field and proper simulation conditions to get the best out of the force field. Although the proper reproduction of the order parameter profile is important in showing the validity of the simulations, one should not forget such characteristic features of the phospholipid molecules as the conformation of the beginning of the chains, as emphasized also by Feller et al. (2000). The relatively low order parameters of the beginnings of the *sn*-2

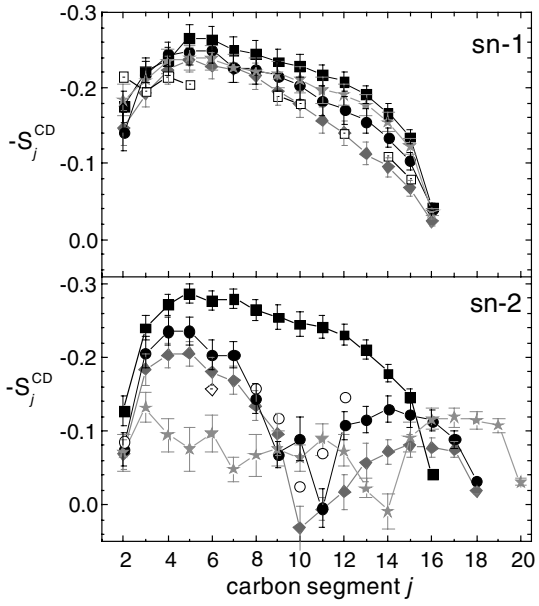

Fig. 5 Averages of the $-S_j^{CD}$ orientational order parameters along the *sn*-1 *(upper panel)* and *sn*-2 *(lower panel)* chains of the DPPC (*filled squares*), POPC (*filled circles*), PLPC (*filled diamonds*), and PAPC (*stars*) bilayers. The standard errors of the mean of the molecular averages are shown as *error bars*. Numbering of the carbon segments is as in Fig. 1. For comparison, the experimental deuterium order parameter profile of the *sn*-1 chain of DPPCs (*open squares*) in a liquid-crystalline phase at 50°C is shown (Seelig and Seelig 1974), together with the scarce experimental values for the *sn*-2 chains of POPC (*open circles*) and PLPC (*open diamonds*) systems (Seelig and Waespe-Sarcevic 1978; Baenziger et al. 1991). Note that owing to the relatively short simulation time, the order parameter values may not have fully converged, as indicated by the *error bars* and the slow decay of the autocorrelation functions in Fig. 6

chains and especially the prevalence of separate order parameters in the C2 position were first reported by Seelig and Seelig (1974). Later, they were related to the distinct prevailing conformation of the beginning of the *sn*-2 chains, which is on average slightly more parallel to the membrane plane than in the *sn*-1 chains (Seelig and Seelig 1980; Douliez et al. 1995), leading to the inequivalence of CH bonds at position C2 (see separate S^{CD} values earlier and the more detailed analysis of inequivalence in Hyvönen et al. 1997b).

As expected, the double bonds induce profound differences in the order parameters along the *sn*-2 chains (Seelig and Seelig 1977; Baenziger et al. 1991). The ordering of the *sn*-2 chains of DPPC is closely similar to that of the *sn*-1 chains. In contrast, the double bonds cause a strong decrease in order parameters, especially in the region of double bonds. In the case of POPC and PLPC, accordance with the scarce experimental values is good (Seelig and Waespe-Sarcevic 1978; Baenziger et al. 1991). For the *sn*-2 chains of PAPC, the effect of four double bonds is so strong that the S^{CD} values vary mostly between 0 and 0.1, in accordance with the ^{2}H NMR and with simulation studies on PCs with six double bonds in their *sn*-2 22:6ω3 docosahexaenoyl

chains (Huber et al. 2002; Feller et al. 2002; Eldho et al. 2003). In the 22:6ω3 chains, however, the double-bond region extends to the very end of the chains, so no increase is observed after the double-bond region, a situation still observable here in the case of PAPC with 20:4ω6 chains, and in accordance with the deuterium order parameters in the case of *sn*-2 22:5ω6 docosapentaenoyl chains (Eldho et al. 2003). To address the origins of the low order parameters of the double-bond regions, the angle distributions of the CH bonds with respect to the bilayer normal were determined (data not shown), which clearly indicate that the methylene hydrogens span the entire possible range of orientations, leading to the low ordering, as has been discussed by Feller et al. (2002). Overall, the features characteristic to the ordering of the unsaturated *sn*-2 chains are well reproduced, although it should be noted that owing to the relatively short simulation time, the order parameter values may not have fully converged, as indicated by the error bars and the slow decay of the autocorrelation functions in Fig. 6, and as discussed later.

The proportion of *gauche* conformations and the isomerization rate of the bonds along the chains were also determined (data not shown). In general, the percentage of single bonds in *gauche* states falls between roughly 20 and 30% corresponding to approximately 3–4 *gauche* bonds per chain, in good accordance with the estimates for DPPC from Fourier transform IR spectroscopy (Mendelsohn et al. 1991). The beginnings of the chains induce an increase, together with the double bonds. Specifically, the beginning of the *sn*-2 chain has approximately 50% of the bonds over carbons C2-C3 in the *gauche* state. The single bonds that are nearest to double bonds without being conjugated to a double-bonded carbon are more than 30% in the *gauche* state. A small increase in the number of *gauche* states towards the chain ends was observable, with a percentage of approximately 30% in the end in all systems and in both chains.

The isomerization rate of around 30 ns^{-1} is the usual level in both chains, which gives an estimate of the interval of roughly more than 30 ps between the changes between *gauche* and *trans* states. This level is slightly higher in the DPPC bilayer than in unsaturated layers. The isomerization rate is very low in the beginnings of the chains, on the order of 5 ns^{-1}, and similarly also in the bonds nearest to the *skew* state bonds, which again are those nearest to the double bonds. The *skew* state bonds present remarkably high isomerization rates of up to 150 ns^{-1}. Interestingly, in solid-state NMR experiments the *skew* state bonds have been suggested to be responsible for the flexibility of the polyunsaturated chains (Eldho et al. 2003; Gawrisch et al. 2003).

Correlation functions are conventionally utilized in the characterization of varying relaxation processes in bilayer systems. Here, with the relatively short simulation time, the correlation functions give an impression of the convergence along the molecules and provide information on the short-scale dynamics of varying CH bonds along the chains and in the glycerol backbone and head group (Fig. 6). Of these, the CH bond at the *sn*-3 position of the glycerol backbone shows the slowest

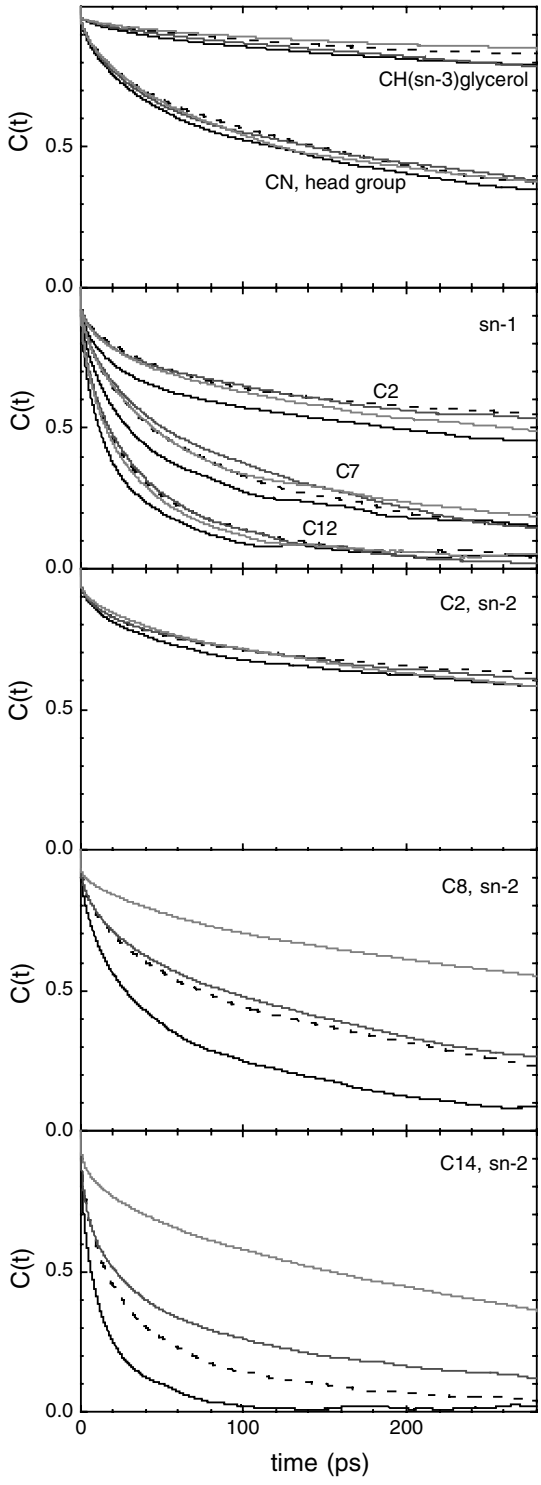

Fig. 6 Correlation functions of CH vectors in the head group (carbon CN in Fig. 1) and at the *sn*-3 position of the glycerol backbone (*top panel*), at various positions along the *sn*-1 chain (*second panel*) and along the *sn*-2 chain (*bottom three panels*) in the four bilayer systems: DPPC (*solid black line*), POPC (*broken line*), PLPC (*dark grey line*) and PAPC (*light grey line*)

relaxation, in accordance with findings in earlier studies considering glycerol as the stiffest part of the PC molecule (Wiener and White 1992). At this time scale, relaxation of all CH bonds is quickest for the saturated DPPC bilayer, which, especially in the case of the glycerol backbone and the head group, may result from the higher simulation temperature.

The correlation function for the CH vectors from the *sn*-1 chains is very similar in all unsaturated bilayers and shows only slightly faster relaxation in the saturated DPPC bilayer. This holds true also at the position of carbon C2 of the *sn*-2 chain. However, at position C8 of the *sn*-2 chain, relaxation is considerably slower in the POPC and PLPC bilayers than in the DPPC bilayer and becomes even slower in the PAPC bilayer. Position C8 in POPC and PLPC bilayers is similar in the sense that this carbon segment is the last before the double bond and is related to the dihedral angles C7-C8 and C8-C9, in which isomerization behaviour is similar in POPC and PLPC bilayers also (data not shown). However, carbon segment C8 is involved in the stiff double bond of the PAPC bilayer, which probably causes the slow decay of its correlation function. Interestingly, the stiffness of the *cis* double bond dominates, causing the slowing of the relaxation despite the flexibility of the rotation of the dihedral angle C7-C8. At the position of carbon C14, the CH vector shows faster relaxation in the order PAPC < sn-1 chain CH bonds, as described by correlation functions, is similar here to that of the simulations of the SDPC bilayer with *sn*-1 stearoyl and *sn*-2 docosahexaenoyl chains, the relaxation of *sn*-2 chain CH bonds is considerably slower (Feller et al. 2002), reflecting, at least, the smaller number of flexible *skew* state bonds in the arachidonoyl chain.

In conclusion, at least short-scale mobility is not directly able to explain the increased passive permeability across the bilayer due to unsaturation. Moreover, the fraction of free volume (Fig. 4) along with increasing unsaturation fails to offer any straightforward explanation. What will be needed is thus an analysis of a free volume that would take into account the shape distribution of the free volume available, together with analysis of the dynamics at longer time scales than in this study. It is possible to suggest, however, plausible pieces of evidence, shown here and by others, which are related to the increased permeability along with the enhanced unsaturation. First, the larger areas per lipid in unsaturated bilayers may reduce the barrier against water molecules reaching the interior parts of the membrane. Second, the heavily increased overlap of the double-bond region and the water phase in the polyunsaturated membranes (Fig. 4) would enhance the possible tendency of double bonds to ferry small molecules, in comparison with that of the monounsaturated and saturated chains (Wiener and White 1992). Thirdly, the exceptional flexibility of the *skew* state bonds, observed here and in studies of *sn*-2 docosahexaenoyl PCs (Feller et al. 2002; Eldho et al. 2003) may play a role in enhancing the diffusion of foreign molecules. Finally, the suggested ability of double bonds to hydrogen-bond (Vorobyov et al. 2002) would directly enhance the possibilities of hydrophilic molecules to transiently reside in the hydrophobic interior of the bilayer. These aspects taken together provide a reasonable explanation for the enhanced permeability, although MD simulations most likely will describe such a phenomenon in detail, as the size and time scales of the MD simulations of lipid membranes are rapidly increasing. Indeed, large-scale simulations have already been performed addressing the effects of anesthetics and their penetration to biological membranes (Koubi et al. 2003; Pasenkiewicz-Gierula et al. 2003). This progress will enable us to more efficiently investigate the properties of variably unsaturated lipid bilayers, together with mixtures of other physiologically important lipids such as sphingomyelins and cholesterol. Such studies will provide us with crucial information on the interactions between physiologically relevant lipid species, also deepening understanding of the biology of specialized membrane regions such as rafts.

Summary

The objective of this study was to elucidate the possible structural effects that an increasing number of double bonds in the *sn*-2 chain of PC molecules has on the membrane structure and short-scale dynamics of molecular parts. Although the results suggest some problems in the CHARMM force field of the lipids when applied in a constant-pressure ensemble, as the area per lipid of the saturated DPPC in the reference simulation was underestimated and the ordering of the saturated chains of unsaturated lipids was overestimated, the features appearing in the ordering of the unsaturated chains are consistent with the behaviour known from ^{2}H NMR experiments. Furthermore, the behaviour of hydrating water and the head groups, as well as the electron density profile and the electrostatic potential are in line with those of earlier experimental and simulation studies. It should be kept in mind, however, that the simulations here were on a nanosecond scale, and therefore not all features are converged on this time scale.

Although the dimensions of the variously unsaturated bilayers do vary, the electron density profiles, together with the properties of the lipid head groups and the hydrating water, are quite similar between the variably unsaturated bilayers on this time scale. However, a few water molecules were seen to incidentally penetrate into the membrane interior of the PAPC bilayer, where the region of double bonds is also shown to span all the way from the centre of the bilayer to the head group region. In general, the ordering of the chains is decreased owing to unsaturation, especially of the unsaturated *sn*-2 chains themselves. The incorporation of double bonds in the *sn*-2 hydrocarbon chain of the PCs reveals the dual nature of the *cis* double bond: these structural units are

themselves rigid, but this is compensated for by the flexibility of the *skew* state single bonds next to double bonds and the increased number of *gauche* states in the single bonds next to the *skew* state single bonds.

Acknowledgements We thank the Finnish IT Center for Science (Espoo, Finland) for computer resources. The Wihuri Research Institute is maintained by the Jenny and Antti Wihuri Foundation. This work was, in part, supported by grants from the Federation of Finnish Insurance Companies and the Academy of Finland (grant number 80851).

References

Akutsu H, Nagamori T (1991) Conformational analysis of the polar head group in phosphatidylcholine bilayers. A structural change induced by cations. Biochemistry 30:4510–4516

Anezo C, de Vries AH, Höltje H-D, Tieleman DP, Marrink S-J (2003) Methodological issues in lipid bilayer simulations. J Phys Chem B 107:9424–9433

Bachar M, Brunelle P, Tieleman DP, Rauk A (2004) Molecular dynamics simulation of a polyunsaturated lipid bilayer susceptible to lipid peroxidation. J Phys Chem B 108:7170–7179

Baenziger JE, Jarrel HC, Hill RJ, Smith ICP (1991) Average structural and motional properties of a diunsaturated acyl chain in a lipid bilayer: effects of two cis-unsaturated double bonds. Biochemistry 30:894–903

Bandyopadhyay S,Tarek M, Klein ML (1998) Computer simulation studies of amphiphilic interfaces. Curr Opin Colloid Interface Sci 3:242–246

Berendsen HJC,Tieleman DP (1998) Molecular dynamics: studies of lipid bilayers. In: Encyclopedia of computational chemistry. Wiley, London, pp 1639–1650

Berger O, Edholm O, Jähnig F (1997) Molecular dynamics simulations of a fluid bilayer of dipalmitoylphosphatidylcholine at full hydration, constant pressure, and constant temperature. Biophys J 72:2002–2013

Birukov KG, Leitinger N, Bochkov VN, Garcia JGN (2004) Signal transduction pathways activated in human pulmonary endothelial cells by OxPAPC, a bioactive component of oxidized lipoproteins. Microvasc Res 67:18–28

Brooks BR, Bruccoleri RE, Olafson BD, States DJ, Swaminathan S, Karplus M (1983) CHARMM: a program for macromolecular energy, minimization, and dynamics calculations. J Comput Chem 4:187–217

Ceccarelli M, Marchi M (1998) Molecular dynamics simulation of POPC at low hydration near the liquid crystal phase transition. Biochimie 80:415–419

Darden T, York D, Pedersen LG (1993) Particle mesh Ewald: an N log(N) method for Ewald sums in large systems. J Chem Phys 98:10089–10092

Demel RA, Geurts van Kessel WSM, van Deenen LLM (1972) The properties of polyunsaturated lecithins in monolayers and liposomes and the interactions of these lecithins with cholesterol. Biochim Biophys Acta 266:26–40

Douliez J-P, Leonard A,Dufourc EJ (1995) Restatement of order parameters in biomembranes: Calculation of C-C bond order parameters from CD quadrupolar splittings. Biophys J 68:1727–1739

Eldho NV, Feller SE, Tristam-Nagle S, Polozov IV,Gawrisch K (2003) Polyunsaturated docosahexaenoic vs docosapentaenoic acid—differences in lipid matrix properties from the loss of one double bond. J Am Chem Soc 125:6409–6421

Essmann U, Berkowitz ML (1999) Dynamical properties of phospholipid bilayers from computer simulation. Biophys J 76:2081–2089

Essmann U, Perera L, Berkowitz ML, Darden T, Lee H, Pedersen LG (1995) A smooth particle mesh Ewald method. J Chem Phys 103:8577–8593

Esterbauer H, Dieber-Rotheneder M, Waeg G, Striegl G, Jürgens G (1990) Biochemical, structural and functional properties of oxidized low-density lipoprotein. Chem Res Toxicol 3:77–92

Evans RW, Williams MA, Tinoco J (1987) Surface areas of 1-palmitoyl phosphatidylcholines and their interactions with cholesterol. Biochem J 245:455–462

Feller SE (2000) Molecular dynamics simulations of lipid bilayers. Curr Opin Colloid Interface Sci 5:217–223

Feller SE, MacKerell AD Jr (2000) An improved empirical potential energy function for molecular simulations of phospholipids. J Phys Chem B 104:7510–7515

Feller SE, Zhang Y, Pastor Y, Brooks BR (1995) Constant pressure molecular dynamics simulation: the Langevin piston method. J Chem Phys 103:4613–4621

Feller SE, Pastor M, Rojnuckarin A, Bogusz S, Brooks BR (1996) Effect of electrostatic force truncation on interfacial and transport properties of water. J Phys Chem 100 :17011–17020

Feller SE, Gawrisch K, MacKerell AD Jr (2002) Polyunsaturated fatty acids in lipid bilayers: intrinsic and environmental contributions to their unique physical properties. J Am Chem Soc 124:318–326

Fettiplace R, Haydon DA, (1980) Water permeability of lipid membranes. Physiol Rev 60:510–550

Flewelling R, Hubbell W (1986) The membrane dipole potential in a total membrane potential model. Applications to hydrophobic ion interactions with membranes. Biophys J 49:541–552

Gawrisch K, Ruston D, Zimmerberg J, Parsegian VA, Rand RP, Fuller N (1992) Membrane dipole potentials, hydration forces, and the ordering of water at membrane surfaces. Biophys J 61:1213–1223

Gawrisch K, Eldho NV, Holte LL (2003) The structure of DHA in phospholipid membranes. Lipids 38:445–452

Heller H, Schaefer M, Schulten K (1993) Molecular dynamics simulation of a bilayer of 200 lipids in a gel and in the liquid-crystal phase. J Phys Chem 97:8343–8360

Holte LL, Senaka AP, Sinnwell T, Gawrisch K (1995) ^{2}H nuclear magnetic resonance order parameter profiles suggest a change of molecular shape for phosphatidylcholines containing a polyunsaturated acyl chain. Biophys J 68:2396–2403

Hoover WG (1985) Canonical dynamics: equilibrium phase-space distributions. Phys Rev A 31:1695–1697

Huang P, Perez JJ, Loew GH (1994) Molecular dynamics simulations of phospholipid bilayers. J Biomol Struct Dyn 11:927–956

Huber T, Rajamoorthi K, Kurze V, Beyer K, Brown MF (2002) Structure of docosahexaenoic acid-containing phospholipid bilayers studied by ^{2}H NMR and molecular dynamics simulations. J Am Chem Soc 124:298–309

Huster D, Jin AJ, Arnold K, Gawrisch K (1997) Water permeability of polyunsaturated lipid membranes measured by ^{17}O NMR. Biophys J 73:855–864

Hyvönen MT, Kovanen PT (2003) Molecular dynamics simulation of sphingomyelin bilayer. J Phys Chem B 107:9102–9108

Hyvönen MT, Ala-Korpela M, Vaara J, Rantala TT,Jokisaari J (1995) Effects of two double bonds on the hydrocarbon interior of a phospholipid bilayer. Chem Phys Letters 246:300–306

Hyvönen MT, Rantala TT,Ala-Korpela M (1997a) Structure and dynamic properties of diunsaturated 1-palmitoyl-2-linoleoyl-*sn*-glycero-3-phosphatidylcholine lipid bilayer from molecular dynamics simulation. Biophys J 73:2907–2923

Hyvönen MT, Ala-Korpela M, Vaara J,Rantala TT,Jokisaari J (1997b) Inequivalence of single CH_a and CH_b methylene bonds in the interior of a diunsaturated lipid bilayer from a molecular dynamics simulation. Chem Phys Lett 268:55–60

In't Veld G, Driessen AJM, Konings WN (1992) Effect of the unsaturation of phospholipid acyl chains on leucine transport of *Lactococcus lactis* and membrane permeability. Biochim Biophys Acta 1108:31–39

Jensen MO, Mouritsen OG, Peters GH (2004) Simulations of a membraneanchored peptide: structure, dynamics, and influence on bilayer properties. Biophys J 86:3556–3575

Jorgensen WL, Chandrasekhar L, Madura JD, Impey RW, Klein ML (1983) Comparison of simple potential functions for simulating liquid water. J Chem Phys 79:926–935

Koenig BW, Strey HH,Gawrisch K (1997) Membrane lateral compressibility determined by NMR and X-ray diffraction: effect of acyl chain polyunsaturation. Biophys J 73:1954–1966

Koubi L, Saiz L, Tarek M,Scharf D, Klein ML (2003) Influence of anesthetic and nonimmobilizer molecules on the physical properties of a polyunsaturated lipid bilayer. J Phys Chem B 107:14500–14508

Marrink S-J, Jähnig F, Berendsen HJC (1996b) Proton transfer across transient single-file water pores in a lipid membrane studied by molecular dynamics simulations. Biophys J 71:632–647

Marrink SJ, Sok RM, Berendsen HJC (1996a) Free volume properties of a simulated lipid membrane. J Chem Phys 104:9090–9099

McIntosh TJ, Simon SA (1986) Hydration force and bilayer deformation: A reevaluation. Biochemistry 25:4058–4066

McIntosh TJ, Simon SA, Needham D, Huang C (1992) Interbilayer interactions between sphongomyelin and sphingomyeli/cholesterol bilayers. Biochemistry 31:2020–2024

Mendelsohn R, Davies MA, Schuster HF, Zu ZG, Bittman R (1991) CD_2 rocking modes as quantitative infrared probes of one-, two-, and three-bond conformational disorder in dipalmitoylphosphatidylcholine and dipalmitoylphosphatidylcholine/cholesterol mixtures. Biochemistry 30:8558–8563

Merz KM Jr (1997) Molecular dynamics simulations of lipid bilayers. Curr Opin Struct Biol 7:511–517

Mitchell DC, Litman BJ (1998) Molecular order and dynamics in bilayers consisting of highly polyunsaturated phospholipids. Biophys J 74:879–891

Murzyn K, Rog T, Jezierski G, Takaoka Y, Pasenkiewicz-Gierula M (2001) Effects of phospholipid unsaturation on the membrane/water interface: a molecular simulation study. Biophys J 81:170–183

Nagle JF, Tristam-Nagle S (2000) Structure of lipid bilayers. Biochim Biophys Acta 1469:159–195

Pasenkiewicz-Gierula M, Rog T, Grochowski J,Serda P, Czarnecki R, Librowski T, Lochynski S (2003) Effects of a carane derivative local anesthetic on a phospholipid bilayer studied by molecular dynamics simulation. Biophys J 85:1248–1258

Pastor RW (1994) Molecular dynamics and Monte Carlo simulations of lipid bilayers. Curr Opin Struct Biol 4:486–492

Patra M, Karttunen M, Hyvönen MT, Falck E, Lindqvist P, Vattulainen I (2003) Molecular dynamics simulations of lipid bilayers: major artifacts due to truncating electrostatic interactions. Biophys J 84:3636–3645

Peterson U, Mannock DA,Lewis RNAH, Pohl P, McElhaney RN, Pohl EE (2002) Origin of membrane dipole potential: contribution of the phospholipid fatty acid chains. Chem Phys Lipids 117:19–27

Rabinovich AL, Ripatti PO, Balabaev NK, Leermakers FAM (2003) Molecular dynamics simulations of hydrated unsaturated lipid bilayers in the liquid-crystal phase and comparison to self-consistent field modeling. Phys Rev E 67:11909–11923

Rog T, Murzyn K, Gurbiel R, Takaoka Y, Kusumi A, Pasenkiewicz-Gierula M (2004) Effects of phospholipid unsaturation on the bilayer nonpolar region: a molecular simulation study. J Lipid Res 45:326–336

Sachs JN, Nanda H, Petrache HI, Woolf TB (2004) Changes in phosphatidylcholine headgrouptilt anf water order induced by monovalent salts: molecular dynamics simulation. Biophys J 86:3772–3782

Saiz L, Bandyopadhyay S, Klein ML (2001) Towards an understanding of complex biological membranes from atomistic molecular dynamics simulations. Biosci Rep 22:151–173

Saiz L, Klein ML (2001a) Structural properties of a highly polyunsaturated lipid bilayer from molecular dynamics simulations. Biophys J 81:204–216

Saiz L, Klein ML (2001b) Influence of highly polyunsaturated lipid acyl chains of biomembranes on the NMR order parameters. J Am Chem Soc 123:7381–7387

Schamberger J, Clarke RJ (2002) Hydrophobic ion hydration and the magnitude of the dipole potential. Biophys J 82:3081–3088

Schlenkrich M, Brickmann J, MacKerell Jr AD, Karplus M (1996) An empirical potential energy function for phospholipids: criteria for parameter optimization and applications. In: Merz KM Jr , Roux B (eds) Biological membranes: a molecular perspective from computation and experiment. Birkhäuser, Boston, pp 31–81

Seelig A, Niederberger W (1974) Deuterium-labeled lipids as structural probes in liquid-crystalline bilayers: a deuterium magnetic resonance study. J Am Chem Soc 96:2069–2072

Seelig A, Seelig J (1974) The dynamic structure of fatty acyl chains in a phospholipid bilayer measured by deuterium magnetic resonance. Biochemistry 13:4839–4845

Seelig A, Seelig J (1977) Effect of single cis double bond on the structure of a phospholipid bilayer. Biochemistry 16:45–50

Seelig J,Waespe-Sarcevic N (1978) Molecular order in cis and trans unsaturated phospholipid bilayer. Biochemistry 17:3311–3315

Seelig J, Seelig A (1980) Lipid conformation in model membranes and biological membranes. Q Rev Biophys 13:19–61

Shinoda W, Shimizu M, Okazaki S (1998) Molecular dynamics study on electrostatic properties of a lipid bilayer: polarization, electrostatic potential, and the effects on structure and dynamics of water near the interface. J Phys Chem B 102:6647–6654

Simon SA, McIntosh TJ (1989) Magnitude of the solvation pressure depends on dipole potential. Proc Natl Acad Sci USA 86:9263–9267

Stillwell W, Wassal SR (2003) Docosahexaenoic acid: membrane properties of a unique fatty acid. Chem Phys Lipids 126:1–27

Tieleman DP, Marrink S-J,Berendsen HJC (1997) A computer perspective of membranes: molecular dynamics studies of lipid bilayer systems. Biochim Biophys Acta 1331:235–270

Tobias DJ, Tu K, Klein ML (1997) Atomic-scale molecular dynamics simulations of lipid membranes. Curr Opin Colloid Interface Sci 2:15–26

Tomita M, Baker RC, Ando S, Santoro TJ (2004) Arachidonoylphospholipid remodeling in proliferating murine T cells. Lipids Health Dis 3:1–12

Venable RM, Pastor RW (2002) Molecular dynamics simulation of water wires in a lipid bilayer and water/octane model systems. J Chem Phys 116:2663–2664

Vorobyov I, Yappert MC, DuPre DB (2002) Energetic and topological analyses of cooperative sH and pH-bonding interactions. J Phys Chem A 106:10691–10699

Walter L, Stella N (2003) Endothelin-1 increases 2-arachidonoyl glycerol (2-AG) production in astrocytes. Glia 44:85–90

Walton KA, Hsieh X, Gharavi N, Wang S, Wang G, Yeh M, Cole AL, Berliner JA (2003) Receptors involved in the oxidized 1-palmitoyl-2-arachidonoylsn-glycero-3-phosphorylcholine-mediated synthesis of interleukin-8. J Biol Chem 278:29661–29666

Wiener MC, White SH (1992) Structure of a fluid dioleoylphosphatidylcholine bilayer determined by joint refinement of X-ray and neutron diffraction data. III. Complete structure. Biophys J 61:434–447

Zeng Y,Han X,Gross RW (1998) Phospholipid subclass specific alterations in the passive ion permeability of membrane bilayers: separation of enthalpic and entropic contributions to transbilayer ion flux. Biochemistry 37:2346–2355